Geomechanics and Engineering, *Vol. 11, No. 1 (2016) 117-139*
DOI: http://dx.doi.org/10.12989/gae.2016.11.1.117

Deformation analyses during subway shield excavation considering stiffness influences of underground structures

Zhi-guo Zhang [*1,2,3], Qi-hua Zhao [2a] and Meng-xi Zhang [4b]

[1] *School of Environment and Architecture, University of Shanghai for Science and Technology, 516 Jungong Road, Shanghai 200093, China*
[2] *State Key Laboratory of Geohazard Prevention and Geoenvironment Protection, Chengdu University of Technology, Chengdu 610059, China*
[3] *Key Laboratory of Geohazard Prevention of Hilly Mountains, Ministry of Land and Resources, Fuzhou 350002, China*
[4] *Department of Civil Engineering, Shanghai University, Shanghai 200072, China*

(*Received August 25, 2015, Revised February 15, 2016, Accepted April 01, 2016*)

Abstract. Previous studies for soil movements induced by tunneling have primarily focused on the free soil displacements. However, the stiffness of existing structures is expected to alter tunneling-induced ground movements, the sheltering influences for underground structures should be included. Furthermore, minimal attention has been given to the settings for the shield machine's operation parameters during the process of tunnels crossing above and below existing tunnels. Based on the Shanghai railway project, the soil movements induced by an earth pressure balance (EPB) shield considering the sheltering effects of existing tunnels are presented by the simplified theoretical method, the three-dimensional finite element (3D FE) simulation method, and the in-situ monitoring method. The deformation prediction of existing tunnels during complex traversing process is also presented. In addition, the deformation controlling safety measurements are carried out simultaneously to obtain the settings for the shield propulsion parameters, including earth pressure for cutting open, synchronized grouting, propulsion speed, and cutter head torque. It appears that the sheltering effects of underground structures have a great influence on ground movements caused by tunneling. The error obtained by the previous simplified methods based on the free soil displacements cannot be dismissed when encountering many existing structures.

Keywords: shield tunneling; stiffness influence; shield propulsion parameters; simplified theoretical method; 3D FE numerical simulation; case study

1. Introduction

With the rapid improvement of China's economy and growing urbanization, the contradiction between urban development and land shortage has become prominent. As a result, the utilization of underground space has been an important direction of sustainable development. The construction for transportation infrastructures such as subways and railways has reached a new

*Corresponding author, Associate Professor, Post Doctor, E-mail: zgzhang@usst.edu.cn
[a] Professor, E-mail: zhqh@cdut.edu.cn
[b] Professor, E-mail: mxzhang@shu.edu.cn

Copyright © 2016 Techno-Press, Ltd.
http://www.techno-press.org/?journal=gae&subpage=7 ISSN: 2005-307X (Print), 2092-6219 (Online)

peak. However, due to the restriction of underground existing structures such as piles, municipal pipelines and subway tunnels and many other sheltering factors, the new tunnels often inevitably cross over the existing structures. In such sheltering environment, significant construction risks will be encountered during the tunneling process and potential safety hazards will also exist in the existing tunnels. Therefore, it is necessary to have a comprehensive understanding of the sheltering displacements for surrounding soils and the deformation for underground structures during subway shield excavation.

Recently, some attempts have been made to research the response analyses of surrounding soils and existing tunnels due to adjacent tunneling. Methods for solving the problem may be classified into three categories: physical model tests, simplified theoretical methods, and numerical simulated methods. Physical model tests, such as, centrifuge modeling, have served an important role in investigating the interaction mechanisms between existing pipelines (tunnels) and newly built tunnels (Kim *et al*. 1998, Vorster *et al*. 2005a, Byun *et al*. 2006, Lee *et al*. 2006, Marshall *et al*. 2010, Ng *et al*. 2013, Li *et al*. 2014). Another major method used to solve the problem is the simplified theoretical analysis. According to the ground settlement research, Peck (1969) creatively proposed the calculation method based on an empirical relationship, which assumes that the transverse surface settlement profile follows a normal probability curve. In addition, some analytical solutions for estimating soil deformation caused by tunneling have been presented (Verruijt and Booker 1996, Loganathan and Poulos 1998, Bobet 2001, Chou and Bobet 2002, Park 2004, 2005, Yang *et al*. 2004, Bobet 2010, Yang and Wang 2011, Zhang *et al*. 2011, 2014). According to the tunnel-soil-pipeline interaction research, several analytical methods have been employed to predict tunnelling-induced pipeline deformation (Klar *et al*. 2005, 2007, 2008, Vorster *et al*. 2005b). Although the simplified theoretical method is generally not considered the complex excavation process of tunneling, it can reflect the arbitrary ground loss, which is the main reason for the deformation of adjacent pipelines affected by tunneling. Comparatively, the numerical simulated method can take full account of the complex construction sequence and the soil elastoplastic characters. The commercial software will be generally needed in order to form the complex element discrete model. The predication of tunneling-induced ground settlements has been carried out with the finite element method (Thomas and Gunther 2006, Dang and Meguid 2008, Mašín 2009, Gui and Chen 2013, Do *et al*. 2014). The finite element method is also conducted to investigate the deformation of existing tunnels (pipelines) induced by tunnel excavation (Addenbrooke and Potts 2001, Ng *et al*. 2004, Chehade and Shahrour 2008, Liu *et al*. 2009, Wang *et al*. 2011, Ng *et al*. 2013). The simulation of tunnel excavation can be achieved by the birth-death elements after obtaining the initial soil gravity field, and the simulation of soil stress release of tunnel opening can be conducted by supplying the opposite sign of equivalent excavated boundary nodal force. In that case, the finite element method can effectively achieve detailed simulation of the actual tunnel construction process.

The aforementioned simplified theoretical methods to predict the tunneling-induced ground deformation have primarily focused on free soil displacements, and less works have been devoted to the soil movements with taking into account the sheltering effects caused by adjacent underground structures. The previous solutions of the authors (Zhang *et al*. 2011, 2014) are only applied to the free soil displacements induced by tunneling. Actually, in most cases of urban subway construction, buried pipelines, existing tunnels and other sheltering structures have hindered the space and alignment of the new tunnels because of dense buildings and developed networks of subway tunnels. Then the new tunnels often inevitably cross over the structures. Since the stiffness of existing structures is expected to alter tunneling-induced soil movements, the

sheltering influences for underground structures should be included in the analyses in order to realistically predict ground movements caused by shield construction.

In addition, the previous researches for the deformation of existing tunnels (pipelines) induced by tunneling are mostly focused on the interaction between twin parallel or perpendicularly crossing cases. However, there has very little investigation into the problem of over passing and under passing existing tunnels. Compared to parallel or perpendicularly crossing tunnels, there are more influence factors which contribute to the interactions between overlapping tunnels and existing tunnels, especially for crossing above and below cases. Therefore, more studies are needed to investigate the deformation of existing tunnels induced by shield tunneling when tunnels pass over or under each other.

The evaluation of sheltering influences has great importance during the preliminary design phase of a tunneling project, particularly when the plan and profile of the tunnel are under design. As a result, introducing simplified theoretical methods to account for the sheltering influences could be a useful tool for decision making in this phase. Furthermore, a set of engineering protection measurements during the detail design phase should be conducted to assure the safety and serviceability of existing tunnels during tunnel construction.

A tunneling case of the second-stage north route of Shanghai railway transportation line 11 is presented in this study. Considering the sheltering effects of existing tunnels of line 4 during crossing above and below process, the soil movements induced by shield line 11 are presented by using the simplified theoretical method, the 3D FE numerical simulation method, and the in-situ monitoring method. The comparison analysis in detail is conducted between the ground deformation considering sheltering effects and those considering free soil displacements. Meanwhile, the deformation prediction of subway tunnels during complex crossing process is also presented. Furthermore, based on the in-situ monitoring data, the deformation controlling measurements considering sheltering effects are proposed.

2. Engineering background

The second-stage north route of Shanghai railway transportation line 11 extends from Huashan Road to Luoshan Road and thirteen stations are set in plan. The whole length of this route is about 20.89 km, which passes through four districts, including Changning, Xuhui, Pudong New Area and Nanhui. The transit tunnel from Xujiahui station to Shanghai Gymnasium station is a critical part of the second-stage north route of line 11. The up-line tunnel of this section comprises a total length of 1612.909 m and a 0.626 m long-chain, which starts from SDK34+871.716 to SDK36+483.999 in the mileage. The down-line comprises a total length of 1606.956 m and a 5.128 m short-chain, which starts from XDK34+871.716 to XDK36+483.800 in the mileage. The plan view of second-stage north route of Shanghai railway transportation line 11 is shown in Fig. 1.

A connected aisle with a pump room is co-located in this section. This transit tunnel is outfitted with two domestic earth pressure balance (EPB) shield machines. The shield tunneling machine is a slurry earth pressure balance-type machine with an outside diameter of 6.34 m. The designing of the screw conveyor and blowout preventer for EPB shield, which forms two gates controlled by mechanical and manual type, respectively, can greatly reduce the ground loss when suffered adverse soil formations. The up- and down-line shields begin from the south shaft of Xujiahui station and subsequently extend to Shanghai Gymnasium station from north to south. The up-line shield, which takes the lead out of the hole, covers a distance of approximately 100 rings with the

down-line shield. The shield line 11 obliquely crosses the existing tunnels of line 4 with a 75° angle, which belongs to large angle obliquely crossing case. The tunnel lining uses the reinforced concrete which is a universal ring wedge segment. The outside diameter of the segment is 6.2 m and the inner diameter is 5.5 m. The ring width is 1.2 m and the segment thickness is 0.35 m.

As shown in Fig. 2, a special working condition of sheltering tunneling would be encountered when the shield line 11 obliquely crosses the existing tunnels of line 4 in below and above directions successively. The up-line shield crosses below line 4 and the minimum clear distance between the up-line shield and line 4 is 1.82 m, and the down-line shield crosses above line 4 and the minimum clear distance between the down-line shield and line 4 is 1.69 m. The covering soil depth of down-line tunnel is 6 m. The horizontal distance between the centers of double-twin tunnels is 4 m.

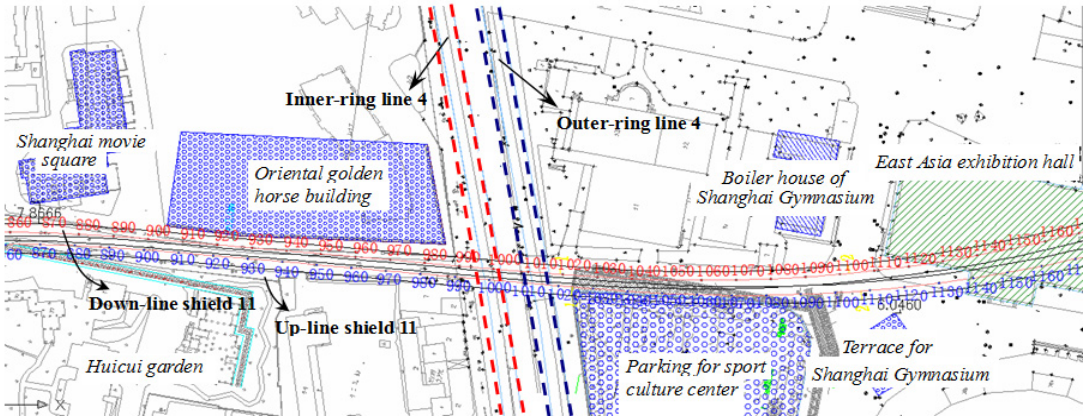

Fig. 1 Plan view of second-stage north route of Shanghai railway transportation line 11

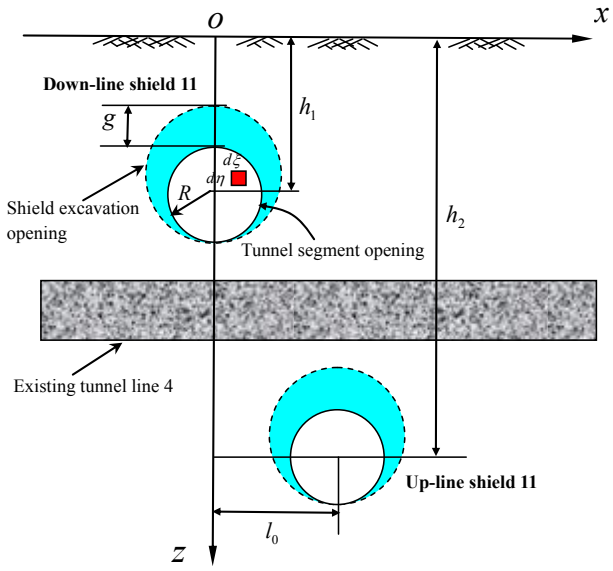

Fig. 2 Sectional view for sheltering case in this project

Table 1 Geotechnical parameter for in-situ soil

Layer No.	Soil name	Thickness (m)	Unit weight γ (kN/m^3)	Compression modulus E_s (MPa)	Poisson's ratio v	Cohesion C (kPa)	Friction angle φ (°)
①$_1$	Backfill	2.0	18.0	8.86	0.33	0	22.0
②	Silty clay	1.3	18.5	4.48	0.32	26.0	17.0
③	Muddy silty clay	3.3	17.4	2.54	0.32	10.0	16.5
④	Muddy clay	8.4	16.7	2.09	0.33	11.0	12.5
⑤$_1$	Clay	1.0	17.8	3.36	0.26	14.0	14.5
⑤$_{1a}$	Sandy silt	4.5	18.2	8.21	0.24	5.0	33.0
⑤$_1$	Clay	4.3	17.8	3.36	0.26	14.0	14.5
⑤$_3$	Silty clay	15.0	18.1	4.66	0.29	16.0	22.5

The tunneling geology is characterized by coastal plain topography, which primarily consists of saturated cohesive soil and silty soil. The soils in situ can be divided into eight layers. The soil geotechnical properties and main physical mechanical parameters are shown in Table 1. The soils surrounding the shield tunnels predominantly consist of muddy clay and silty clay and exhibit the following characteristics: large void ratio, high plasticity, poor permeability, high water content, low shear strength, and low modulus of deformation. It can be seen that the construction site exists complex stratum, and the extreme accidences may be occurred according to the ultra closed distance between structures and the shallow covering soil excavation.

3. Simplified theoretical method for sheltering soil movements induced by tunneling

The stochastic medium theory is utilized in this study to predict the arbitrary soil movements caused by shield excavation of line 11 considering the sheltering effects of existing line 4. The stochastic medium theory has been used to predict the ground surface movements induced by tunneling and mining (Liu 1993, Yang *et al*. 2004, Yang and Wang 2011). According to the stochastic medium theory, it is assumed that an underground excavation can be divided into infinitesimal excavation elements and that the soil movements caused by the excavation equals the sum of the movements due to each elemental excavation. Currently the stochastic medium theory is mainly used to predict tunneling-induced free soil displacements and ground surface settlements, but the sheltering effects of existing underground structures and arbitrary subsoil movements are not considered. Therefore, it still needs to estimate the arbitrary subsoil deformation by the modified stochastic medium method in order to investigate the sheltering effects.

According to the excavation element system, the origin of calculation coordinate is assumed at the ground surface and it is shown as Fig. 2. The stratum corresponds to the global coordinate (x, y, z), while the excavation adopts the local coordinate (ξ, ζ, η). The dimension of excavation element is defined as $d\xi$, $d\zeta$ and $d\eta$. By assuming that every excavation element collapses completely in the whole excavation zone Ω, the arbitrary soil horizontal displacements $u(x, z)$ and arbitrary soil settlements $w(x, z)$ can be obtained by the applying superposition principle, i.e.

$$u(x,z)=\iint_{\Omega}\frac{(x-\xi)\tan\beta}{(\eta-z)^2}\exp\left[-\frac{\pi\tan^2\beta}{(\eta-z)^2}(x-\xi)^2\right]d\xi d\eta \tag{1}$$

$$w(x,z)=\iint_{\Omega}\frac{\tan\beta}{\eta-z}\exp\left[-\frac{\pi\tan^2\beta}{(\eta-z)^2}(x-\xi)^2\right]d\xi d\eta \tag{2}$$

where β is the principal influence angle of tunnel excavation deformation, whose value depends on the stratigraphic conditions of excavation and the sheltering degree of existing structures. It should be noted that the above-mentioned formula can also estimate the free soil displacements on the condition of the parameter β without considering the sheltering effects. When the coordinate value $z = 0$, the results of Eqs. (1) and (2) are the ground surface horizontal displacements and vertical displacements, respectively.

As shown in Fig. 2, taking the down-line 11 for example, the non-uniform convergence displacement model is set to the tunnel opening. The initial cross-section area of shield excavation is denoted by Ω, and Φ is the cross-section area of formed tunnels after the segment assembly is completed. Then the radial convergence is $\Delta A = \Omega - \Phi$, the arbitrary soil horizontal displacements $u_0(x, z)$ and soil settlements $w_0(x, z)$ induced by the difference ΔA can be estimated as

$$u_0(x,z)=\iint_{\Omega-\Phi}\frac{(x-\xi)\tan\beta}{(\eta-z)^2}\exp\left[-\frac{\pi\tan^2\beta}{(\eta-z)^2}(x-\xi)^2\right]d\xi d\eta \tag{3}$$

$$w_0(x,z)=\iint_{\Omega-\Phi}\frac{\tan\beta}{\eta-z}\exp\left[-\frac{\pi\tan^2\beta}{(\eta-z)^2}(x-\xi)^2\right]d\xi d\eta \tag{4}$$

The previous studies (Lee *et al*. 1992, Chehade and Shahrour 2008) indicate that the tunneling-induced soil deformation is primarily caused by the ground loss. Lee *et al*. (1992) used the gap parameter to measure the ground loss. It is considered that the gap parameter g primarily consists of the physical gap G_p between the outer skin of the shield and the tunnel lining, the elasto-plastic deformation U_{3D} at the tunnel excavation face, and the over-excavation value ψ, which denotes the quality of workmanship. Thus the gap parameter g can be estimated as

$$g = G_p + U_{3D} + \Psi \tag{5}$$

Considering that the shield mechanical properties and engineers operating skills improve continually, the ground loss due to the elasto-plastic deformation U_{3D} and the over-excavation Ψ in Eq. (5) decreases correspondingly. Therefore, the outer diameter difference G_p between shield machine and tunnel lining becomes the main components of gap parameter g. Based on the previous researches (Loganathan and Poulos 1998, Park 2004, 2005), the non-uniform convergence displacement model is adopted for the shield excavation boundary and the gap parameter g is defined in Eq. (5), which is shown in Fig. 2. In fact, an entire sinking of tunnel will happen after the segments installation, while tunnel falls to the bottom of the excavation boundary, which is equivalent to a downward displacement of $g/2$ for the uniform convergence situation. Using this non-uniform convergence displacement model, the arbitrary soil horizontal displacements $u_0(x, z)$ and soil settlements $w_0(x, z)$ induced by the down-line 11 excavation can be obtained

$$u_0(x,z)=\int_{h_1-R-g}^{h_1+R}\int_{-\sqrt{\left(R+g/2\right)^2-\left(h_1-g/2-z\right)^2}}^{\sqrt{\left(R+g/2\right)^2-\left(h_1-g/2-z\right)^2}}\frac{(x-\xi)\tan\beta}{(\eta-z)^2}\exp[-\frac{\pi\tan^2\beta}{(\eta-z)^2}(x-\xi)^2]d\xi d\eta$$
$$-\int_{h_1-R}^{h_1+R}\int_{-\sqrt{R^2-(h_1-z)^2}}^{\sqrt{R^2-(h_1-z)^2}}\frac{(x-\xi)\tan\beta}{(\eta-z)^2}\exp[-\frac{\pi\tan^2\beta}{(\eta-z)^2}(x-\xi)^2]d\xi d\eta \tag{6}$$

$$w_0(x,z)=\int_{h_1-R-g}^{h_1+R}\int_{-\sqrt{\left(R+g/2\right)^2-\left(h_1-g/2-z\right)^2}}^{\sqrt{\left(R+g/2\right)^2-\left(h_1-g/2-z\right)^2}}\frac{\tan\beta}{\eta-z}\exp[-\frac{\pi\tan^2\beta}{(\eta-z)^2}(x-\xi)^2]d\xi d\eta$$
$$-\int_{h_1-R}^{h_1+R}\int_{-\sqrt{R^2-(h_1-z)^2}}^{\sqrt{R^2-(h_1-z)^2}}\frac{\tan\beta}{\eta-z}\exp[-\frac{\pi\tan^2\beta}{(\eta-z)^2}(x-\xi)^2]d\xi d\eta \tag{7}$$

where R is the tunnel radius after the installation of segments is completed, h_1 is the depth of the down-line 11 tunnel axis. It should be noted that the Eqs. (6) and (7) is only for the single-line excavation case.

In order to reflect the sheltering impacts of existing underground structures, the principal influence angle of tunnel excavation deformation β is determined by the back analyses based on the Powell's optimization procedure. According to the optimization procedure, the objective function $f(\tan\beta)$ can be defined as follows

$$f(\tan\beta)=\sum_{i=1}^{m}(u_{0i}-\tilde{u}_{0i})^2+\sum_{i=1}^{n}(w_{0i}-\tilde{w}_{0i})^2 \tag{8}$$

Based on in-situ monitoring scheme, if the monitoring indicator is only for soil settlements, the objective function $f(\tan\beta)$ can be defined

$$f(\tan\beta)=\sum_{i=1}^{n}(w_{0i}-\tilde{w}_{0i})^2 \tag{9}$$

If the monitoring indicator is only for soil horizontal displacements, the objective function $f(\tan\beta)$ can be defined

$$f(\tan\beta)=\sum_{i=1}^{m}(u_{0i}-\tilde{u}_{0i})^2 \tag{10}$$

where m and n are the number of in-situ monitoring points for soil horizontal and vertical displacements, respectively; u_{0i} is the predicted soil horizontal displacements for the monitoring point i; w_{0i} is the predicted soil vertical displacements for the monitoring point i; $\tilde{u}_{0i}$ is the observed soil horizontal displacements for the monitoring point i, $\tilde{w}_{0i}$ is the observed soil vertical displacements for the monitoring point i.

In the calculation process, the initial parameters are selected and a set of results of $x=[\tan\beta]$ is searched quickly and automatically by using the Powell's optimization method so as to let the objective function meet the accuracy requirements. For the tunneling project in this study, the monitoring point values of surface settlements along the propelling direction are used to conduct

Table 2 Observed data for surface settlements

Measured point No.	Settlement value (mm)	Measured point No.	Settlement value (mm)
S925	5.99	S950	4.26
S930	5.28	S955	3.43
S935	4.97	S960	3.06
S940	4.92	S965	2.26
S945	4.87	S971	1.74

the back analysis, which are listed in Table 2. In the monitoring system, the level-controlling net and three base points which are far away from the construction area are established. The second grade leveling is set in the entire measurement system and the positioning measurement method is used to measure the displacements.

According to the surface settlement data shown in Table 2, the results of Powell's optimization back analyses show that when the parameter $\tan\beta = 0.82$, the posterior error ratio value has been reached to 0.163 with satisfactory accuracy requirements. It should be noted that the parameter $\widetilde{w}_{0i}$ in this optimization method is obtained by in-situ monitoring, thus the principal influence angle β reflects the sheltering effects of adjacent underground structures. Therefore, based on the stochastic medium theory and optimization back analyses program, this study establishes a simplified calculation method to estimate the ground movements caused by tunnel construction considering the sheltering effects of existing underground structures.

Actually, the structure stiffness is one of the main factors affecting the sheltering degree. Based on the tunneling project of second-stage of the north route of Shanghai metro line 11, three cases for sheltering effects due to running tunnel line 4 are set as follows: (1) The actual stiffness of the line 4 is EI; (2) assuming the stiffness of the tunnel is $2EI$; (3) assuming the stiffness of the tunnel is $4EI$. The transversal surface settlements and horizontal displacements caused by shield up-line 11 are obtained by the above-mentioned simplified theoretical approach considering the three sheltering cases and the results are shown in Figs. 3 and 4. Furthermore, as shown in Figs. 5 and 6, the transversal subsoil vertical and horizontal displacements caused by shield up-line 11 are calculated by this simplified theoretical method on the condition that the depth of calculation points below the ground surface is 5 m. From these figures, it is concluded that the increase of sheltering degree is in pace with the increase of tunnel stiffness, while the value of soil settlements

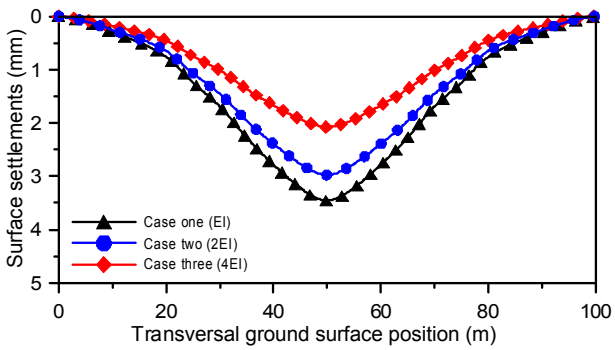

Fig. 3 Comparisons for transverse surface trough with different structure stiffness on condition of $z = 0$ m

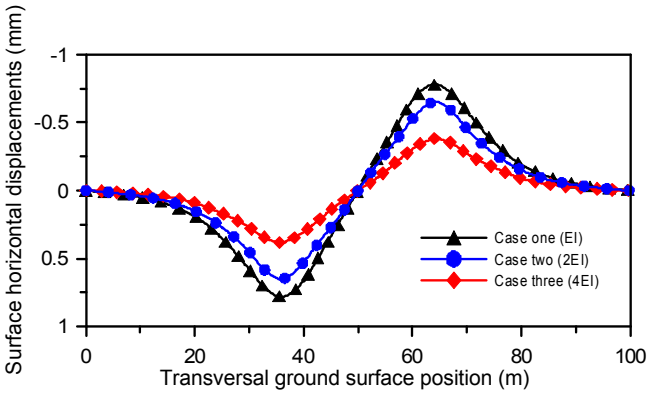

Fig. 4 Comparisons for transverse surface horizontal displacements with different structure stiffness on condition of z = 0 m

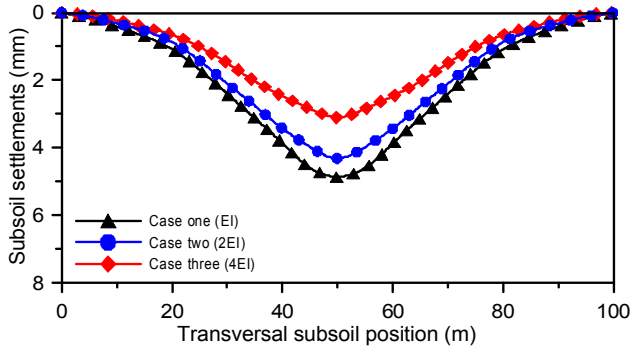

Fig. 5 Comparisons for transverse soil settlements with different structure stiffness on condition of z = 5 m

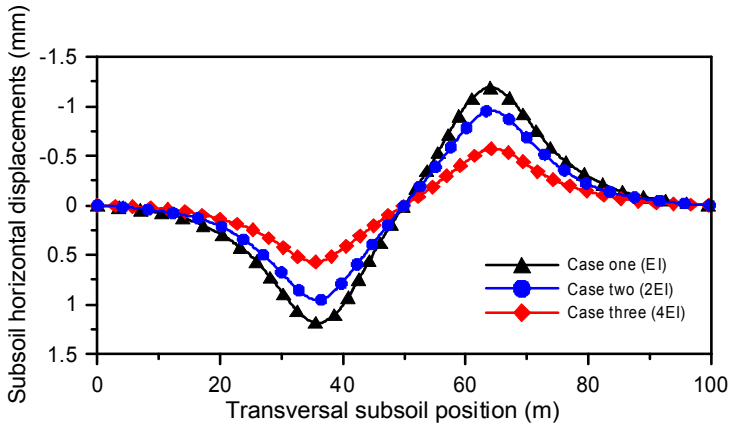

Fig. 6 Comparisons for transverse subsoil horizontal displacements with different structure stiffness on the condition of z = 5 m

and horizontal displacements caused by shield tunnel construction is significantly reduced. It should be noted that the modified stochastic medium method in this study can not only consider surface ground displacements, but also consider arbitrary subsoil movements.

In this study, the arbitrary soil movements caused by double-line shield construction can be calculated by the superposition principle from the single-line shield formula Eqs. (6) and (7). This is because as shown in the study of crossing problems, in order to reduce the construction influence of existing structures and to ensure the shield smooth propelling, the driving of double-line shields (i.e., up- and down-line) is not generally simultaneously. That is, one of the double-line makes the first crossing the existing structures. While the other line would not propel until the monitoring data achieve a certain requirements after the former shield crosses, which can greatly reduce the interaction disturbance effects between double-line shields. In this project the up-line shield takes the lead out of hole and has a distance with down-line shield about 100 rings.

Assuming that the lining radius of up- and down-line tunnel is R, the buried depth of down-line tunnel axis is h_1 and the buried depth of up-line is h_2, the horizontal distance between the double-line tunnel center is l_0. For simplicity, it is supposed that the center position of the down-line tunnel is (0, 0, h_1), as shown in Fig. 2. Thus the arbitrary soil horizontal displacements u_0 (x, z) and soil settlements w_0 (x, z) induced by up- and down-line shield excavation can be expressed as

$$
\begin{aligned}
u_0(x,z) = & \int_{h_2-R-g}^{h_2+R} \int_{-\sqrt{\left(R+g/2\right)^2-\left(h_2-g/2-z\right)^2}-l_0}^{\sqrt{\left(R+g/2\right)^2-\left(h_2-g/2-z\right)^2}-l_0} \frac{(x-\xi)\tan\beta}{(\eta-z)^2} \exp\left[-\frac{\pi\tan^2\beta}{(\eta-z)^2}(x+l_0-\xi)^2\right] d\xi d\eta \\
& - \int_{h_2-R}^{h_2+R} \int_{-\sqrt{R^2-(h_2-z)^2}-l_0}^{\sqrt{R^2-(h_2-z)^2}-l_0} \frac{(x-\xi)\tan\beta}{(\eta-z)^2} \exp\left[-\frac{\pi\tan^2\beta}{(\eta-z)^2}(x+l_0-\xi)^2\right] d\xi d\eta \\
& + \int_{h_1-R-g}^{h_1+R} \int_{-\sqrt{\left(R+g/2\right)^2-\left(h_1-g/2-z\right)^2}}^{\sqrt{\left(R+g/2\right)^2-\left(h_1-g/2-z\right)^2}} \frac{(x-\xi)\tan\beta}{(\eta-z)^2} \exp\left[-\frac{\pi\tan^2\beta}{(\eta-z)^2}(x-\xi)^2\right] d\xi d\eta \\
& - \int_{h_1-R}^{h_1+R} \int_{-\sqrt{R^2-(h_1-z)^2}}^{\sqrt{R^2-(h_1-z)^2}} \frac{(x-\xi)\tan\beta}{(\eta-z)^2} \exp\left[-\frac{\pi\tan^2\beta}{(\eta-z)^2}(x-\xi)^2\right] d\xi d\eta
\end{aligned}
\tag{11}
$$

$$
\begin{aligned}
w_0(x,z) = & \int_{h_2-R-g}^{h_2+R} \int_{-\sqrt{\left(R+g/2\right)^2-\left(h_2-g/2-z\right)^2}-l_0}^{\sqrt{\left(R+g/2\right)^2-\left(h_2-g/2-z\right)^2}-l_0} \frac{\tan\beta}{\eta-z} \exp\left[-\frac{\pi\tan^2\beta}{(\eta-z)^2}(x+l_0-\xi)^2\right] d\xi d\eta \\
& - \int_{h_2-R}^{h_2+R} \int_{-\sqrt{R^2-(h_2-z)^2}-l_0}^{\sqrt{R^2-(h_2-z)^2}-l_0} \frac{\tan\beta}{\eta-z} \exp\left[-\frac{\pi\tan^2\beta}{(\eta-z)^2}(x+l_0-\xi)^2\right] d\xi d\eta \\
& + \int_{h_1-R-g}^{h_1+R} \int_{-\sqrt{\left(R+g/2\right)^2-\left(h_1-g/2-z\right)^2}}^{\sqrt{\left(R+g/2\right)^2-\left(h_1-g/2-z\right)^2}} \frac{\tan\beta}{\eta-z} \exp\left[-\frac{\pi\tan^2\beta}{(\eta-z)^2}(x-\xi)^2\right] d\xi d\eta \\
& - \int_{h_1-R}^{h_1+R} \int_{-\sqrt{R^2-(h_1-z)^2}}^{\sqrt{R^2-(h_1-z)^2}} \frac{\tan\beta}{\eta-z} \exp\left[-\frac{\pi\tan^2\beta}{(\eta-z)^2}(x-\xi)^2\right] d\xi d\eta
\end{aligned}
\tag{12}
$$

4. Simplified theoretical method for existing tunnel deformation induced by tunneling

In the conditions of overlapping tunneling construction, the hypotheses of the deformation of existing tunnels are set as follows: (1) the existing tunnel is assumed as a Winkler foundation beam; (2) the continuously distributed springs are set to simulate the interaction between the tunnel and surrounding soils, which satisfies deformation compatibility condition. Then the longitudinal settlements of existing tunnel w_t (x, z) affected by overlapping tunneling construction can be obtained as

$$EI\frac{d^4 w_t(x,z)}{dx^4} + Kw_t(x,z) = Kw_0(x,z) \tag{13}$$

in which EI is the tunnel bending stiffness; $K$is the subgrade coefficient per unit length of the tunnel, and $K = kD$, k is the subgrade modulus coefficient and it can be estimated by the Vesic (1961), that is

$$k = \frac{0.65E_s}{1-v^2}\sqrt[12]{\frac{E_s D^4}{EI}} \tag{14}$$

where v is the soil Poisson's ratio; E_s is the soil compressive modulus; D is the equivalent coefficient and it can be set as the outer diameter of tunnel. w_0 (x, z) is the free soil settlements caused by shield tunneling, which can be calculated by Eq. (7) for the situation of up-line shield single construction or Eq. (12) for the situation of double-line shield construction. In this study for the existing tunnel deformation, the parameter β is based on the free soil movements and it is different with sheltering displacements.

Eq. (13) belongs to the non-homogeneous fourth order differential equation, and it is difficult to be solved directly. Therefore this study uses the weighted residual method to solve this equation. The Euler-Bernoulli Hermite elements with two nodes and four freedom degrees are introduced to analyze the elastic foundation beam problem. The element interpolation function of vertical displacement (i.e., deflection function) w_t (x, z) can be expressed as

$$\begin{aligned} w_t(x,z) &= N_1\omega_1 + N_2\theta_1 + N_3\omega_2 + N_4\theta_2 = (l^3 - 3lx^2 + 2x^3)\omega_1/l^3 \\ &+ (l^2x - 2lx^2 + x^3)\theta_1/l^2 + (3lx^2 - 2x^3)\omega_2/l^3 + (x^3 - lx^2)\theta_2/l^2 \end{aligned} \tag{15}$$

where ω_1 and θ_1 are the vertical displacement and the rotational displacement of the left node in one tunnel element, respectively; ω_2 and θ_2 are the vertical displacement and the rotational displacement of the right node in one tunnel element, respectively; l is the length of tunnel element.

The matrix form of Eq. (15) can be represented as

$$w_t(x,z) = \{N\}\{w_t\}^e \tag{16}$$

where $\{N\}$ is the interpolation function vector and $\{N\} = \{N_1 \quad N_2 \quad N_3 \quad N_4\}$, $\{w_t\}^e$ is the displacement vector for tunnel element and $\{w_t\}^e = \{\omega_1 \quad \theta_1 \quad \omega_2 \quad \theta_2\}^T$.

Based on the interpolation function, the element stiffness matrix for existing tunnel and foundation spring can be expressed as

$$[K_t]^e = \int_o^l EI\left\{\frac{d^2N}{dx^2}\right\}\left\{\frac{d^2N}{dx^2}\right\}^T dx \tag{17}$$

$$[K_s]^e = \int_0^l K\{N\}\{N\}^T dx \tag{18}$$

where $[K_t]^e$ is the element stiffness matrix for existing tunnel; $[K_s]^e$ is the element stiffness matrix for foundation spring.

Applying the element stiffness matrix in Eqs. (17) and (18), the governing differential equation in Eq. (13) can be converse to the finite element equation by using Galerkin method

$$[K_t]^e\{w_t\}^e + [K_s]^e\{w_t\}^e = \int_0^l K\{N\}w_0(x,z)dx \tag{19}$$

Further the Eq. (19) is expressed as the matrix form of the following

$$([K_t]^e + [K_s]^e)\{w_t\}^e = \{F\}^e \tag{20}$$

where $\{F\}^e$ is the element force vector acting on the existing tunnel induced by overlapped tunneling, that is

$$\{F\}^e = \int_0^l K\{N\}w_0(x,z)dx \tag{21}$$

By collecting the element equation, the tunnel deformation in the conditions of overlapping tunneling construction can be obtained

$$([K_t] + [K_s])\{w_t\} = \{F_t\} \tag{22}$$

where $[K_t]$ and $[K_s]$ are the global stiffness matrix of existing tunnel and ground spring, respectively; $\{F_t\}$is the global matrix of force vector acting the tunnel due to adjacent excavation; $\{w_t\}$ is the global nodal displacement vector, including the nodal vertical displacement and rotational displacement.

For a given set of soil movements induced by tunneling in Eqs. (7) and (12), the deformations of existing tunnel can be determined by solving the Eq. (22), and the bending moments M_t (x, z) obtained from the resulting tunnel deformations can be calculated by

$$M_t(x,z) = -EI\frac{d^2w_t(x,z)}{dx^2} \tag{23}$$

The above-mentioned Eq. (23) can be solved using the finite difference method. That is, the tunnel structure can be divided into n elements with a unit length of l along the axial direction. Assuming the deflection at the midpoint of each element is w_{d1}, w_{d2},……, w_{dn}, respectively, except for the 1th and nth elements, the midpoint bending moments of each remaining elements can be calculated as the differential equation

$$M_{t,i}(x,z) = -\frac{EI}{l^2}[w_{t,(i+1)}(x,z) - 2w_{t,i}(x,z) + w_{t,(i-1)}(x,z)] \tag{24}$$

where $i = 2, 3,..., (n-1)$.

5. 3D FE numerical simulation method and deformation prediction

5.1 3D FE numerical model

A 3D finite element program (ABAQUS) is employed as a numerical tool to predict the sheltering effects of existing tunnels of line 4 during shield line 11 crossing above and below existing tunnels process. The 3D model size is 95 m × 144 m × 120 m. The 120 rings excavation of up- and down- line 11 is respectively considered in this numerical simulation. The total distance of 30 rings from the 951th ring to the 980th ring of double lines is selected for the shield propelling trial process, respectively. The soils are simulated by the hexahedral eight-node element C3D8R and the Drucker-Prager model is used as the soil constitutive model. The physical and mechanical parameters are shown in Table 1.

In the numerical model, the realization of shield excavation and support is achieved by using the birth-death elements. The interaction between the soils and lining is simulated by using the interface elements. The tunnel lining is modeled as linear elastic and the hexahedral eight-node element C3D8R is adopted. The strength of the lining concrete is classified as grade C55. According to the specification, the elastic modulus and Poisson's ratio are 3.55×10^4 MPa and 0.2, respectively. In addition, an equivalent layer is established to reflect the comprehensive influences caused by the shield tail void closure, the effects of grouting filling, and the surrounding soil disturbance by the shield propulsion. Equivalent layer elements use the hexahedral eight-node element C3D8R. According to in-situ monitoring, the equivalent layer density is 1900 kg/m^3, the

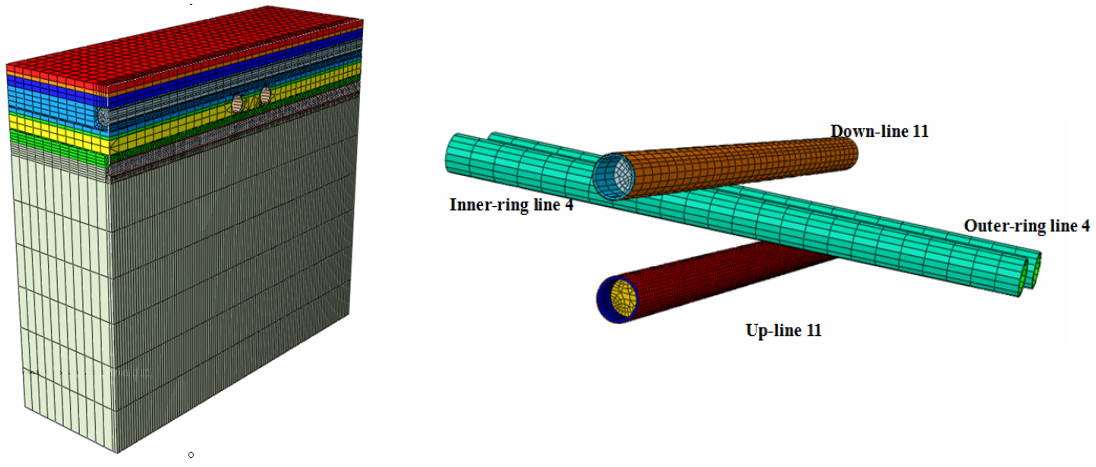

(a) Sectional model along with line 11 direction

(b) Location relationship for shield line 11 and existing tunnel line 4

Fig. 7 3D FE Numerical model for sheltering effects

elastic modulus is 15.5 MPa, the Poisson's ratio is 0.2. The equivalent thickness is set as 105 mm. The sectional model along with the longitudinal axis of the shield line 11 and the discrete model for location relationship between shield line 11 and existing tunnel line 4 are shown in Fig. 7.

In the 3D FE numerical analyses, the shield propelling process can be simulated by changing the element material type in the software, and the stiffness migration method is used to predict the geotechnical influences of overlapping construction. Specifically, the reservation elements are set up in the soil disturbance region around both shield cabinet and segments. When the excavation face is driving forward, the reservation element stiffness in the soil disturbance region is reduced to a very small value (i.e., close to 10^{-6}). Then the lining support start working and the grouting hardness gradually changes. The migration of stiffness and loads can be achieved by activating the pre-set birth-death elements. In this study, the change in modulus of the slurry during the process of hardening involves three stages: an initial period of 0.1 MPa, an interim period of 1 MPa, and a stable period of 10 MPa.

5.2 Sheltering soil displacement prediction and comparisons with different methods

Based on the 3D FE numerical simulation method, the soil settlements on the conditions of the sheltering effects of existing tunnel line 4 and free soil displacements are analyzed comparatively. According to the free soil displacements, because it does not consider the sheltering effects, the numerical model will not simulate the tunnel structures. The property of existing tunnels and equivalent layer can be activated into the properties of surrounding soils. Furthermore, the death elements for the soils inside the tunnel should be activated. In addition, the accuracy of the simplified theoretical method for soil movements considering the sheltering effects is also compared with the 3D FE numerical method.

Considering the sheltering effects of existing tunnel line 4, Fig. 8 shows the transversal surface trough when shield up-line 11 propels to 120th ring (i.e., the up-line shield completes the crossing in this numerical model), which is obtained by the simplified theoretical method (i.e., the modified stochastic medium theory) and 3D FE numerical software, respectively. Meanwhile, the results by the method of Loganathan and Poulos (1998) are also comparatively conducted in Fig. 8. As can be seen, the transverse surface trough curves acquired by the simplified theoretical method are well consistent with the curves obtained by the 3D FE numerical simulation method. It appears that the modified stochastic medium method is a valid approach to estimate the sheltering soil

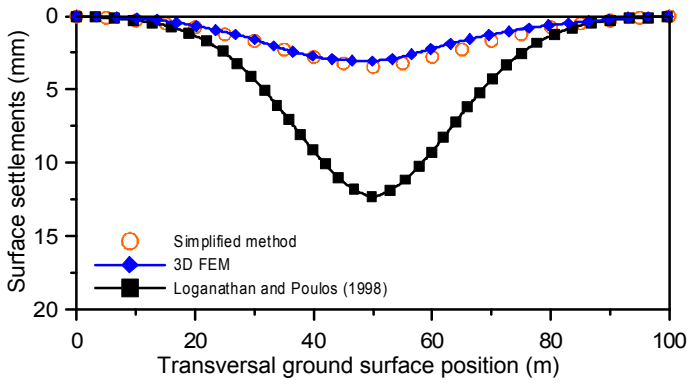

Fig. 8 Comparisons for ground surface transverse trough with different methods

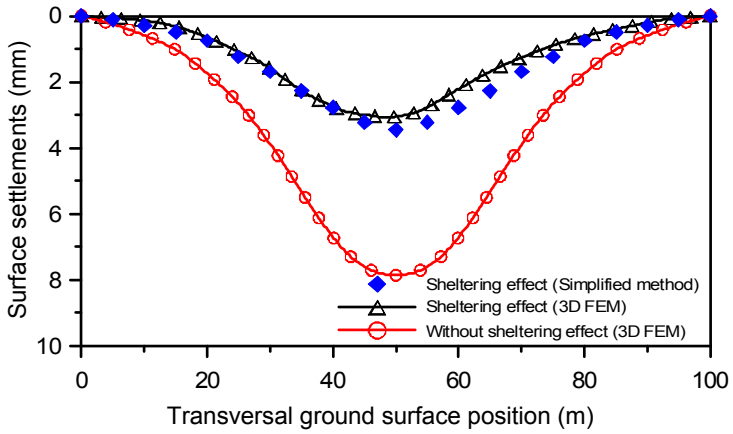

Fig. 9 Comparisons for ground surface settlements due to up-line 11 tunneling (z = 0 m)

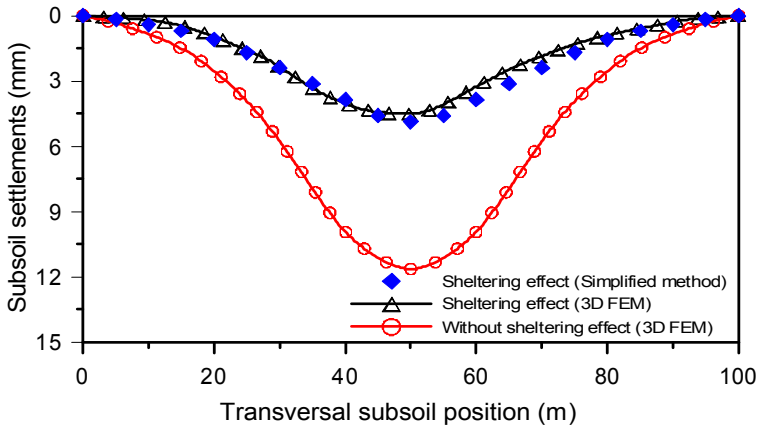

Fig. 10 Comparisons for subsoil settlements due to up-line 11 tunneling whether (z = 5 m)

deformation induced by shield tunneling and the existing underground structures have significant influences on the ground movements. It is also found that the results of using the method of Loganathan and Poulos (1998) have a large difference to the 3D FE numerical method. The reasons may be that, the method of Loganathan and Poulos (1998) is based on the free soil displacements, which does not consider the sheltering effects of existing underground structures. Therefore, the error obtained by the previous simplified methods based on free soil displacements cannot be dismissed when encountering the complex construction environments, especially for lots of existing structures.

Figs. 9 and 10 show the transversal surface settlements and subsoil settlements (the depth below the ground surface is 5 m), respectively, which are obtained by the 3D FE numerical method when shield up-line 11 propels to 120th ring (i.e., the shield up-line completes the crossing) whether considering the sheltering effects of existing line 4 or not. It should be noted that when it does not consider the sheltering effects, the structure stiffness of existing tunnels is no longer activated and the structural properties are set to the properties of surrounding soils. Figs. 11 and 12 show the transversal surface settlements and subsoil settlements (the depth below the ground

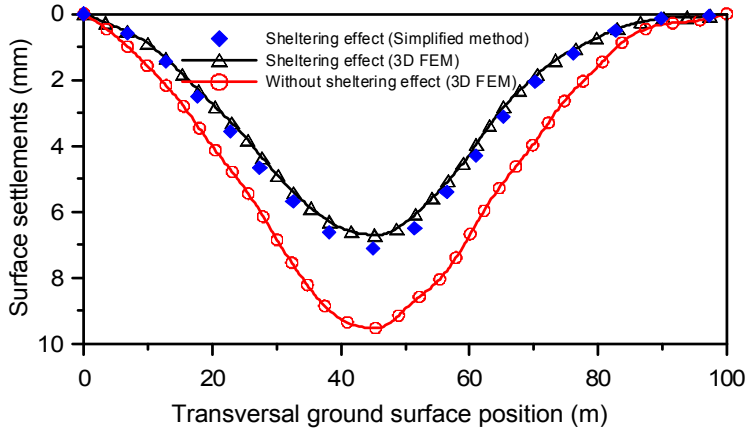

Fig. 11 Comparisons for surface settlements due to up- and down-line 11 tunneling (z = 0 m)

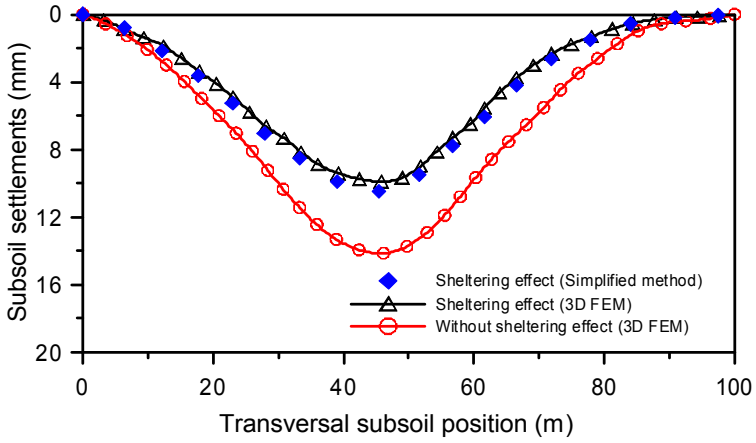

Fig. 12 Comparisons for subsoil settlements due to up- and down-line 11 tunneling (z = 5 m)

surface is 5 m), respectively, which are obtained by using the 3D FE numerical method when shield up- and down-line 11 propel to 120th ring (i.e., the shield up- and down-line complete the crossing) with/without considering the sheltering effects of existing line 4. The above figures show that the solutions without considering the sheltering effects provide larger vertical displacements and overestimate the ground deformation. It is clear that the sheltering effects of existing structures have a greater influence on the soil movements caused by the shield construction, which should be given to emphatic consideration in the theoretical analyses. In addition, the ground surface settlements and subsoil settlements considering the sheltering effects of existing structures by using the simplified theoretical method are also shown in the above-mentioned figures. From these comparisons, it is observed that the good agreement between the solutions from the simplified theoretical method and those from the numerical software is obtained. It appears that the simplified theoretical method based on the modified stochastic medium theory has a high degree of precision to estimate the soil movements induced by shield construction considering the sheltering effects of existing structures.

5.3 Structural deformation prediction and comparisons with different methods

In this study, combined with the in-situ monitoring, the comparative analyses are conducted with two typical cases of the shield up-line 11 propulsion to 120th ring (i.e., up-line propulsion is completed) and the shield down-line 11 propulsion to 120th ring after the crossing completion of the shield up-line 11 (i.e., the up- and down-line shield overlapping crossing is completed). Figs. 13 and 14 shows the vertical deformation values of the inner-ring tunnel line 4, which are acquired by using the simplified theoretical method and the 3D FE numerical software, meanwhile the comparative study with the in-situ monitoring date is also conducted. The vertical displacements of the inner-ring tunnel line 4 induced by the shield up-line 11 propulsion is shown in Fig. 13. From this figure, the maximum displacement value by using the numerical software is 0.26 mm smaller than the value by using the simplified theoretical method. The vertical deformation of the inner-ring tunnel line 4 induced by the overlapping propulsion of up- and down-line shield is shown in Fig. 14. From this figure, the largest deformation value is 1.64 mm by using the simplified method, while by using the 3D FE numerical simulation method, the value is 1.5 mm and there is only 0.14 mm difference. It is clear that the predictions from the simplified theoretical

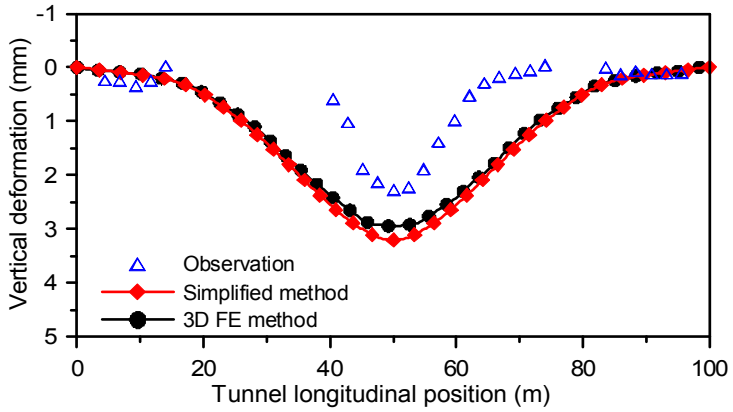

Fig. 13 Comparisons for tunnel vertical deformation after traversing completion for up-line 11

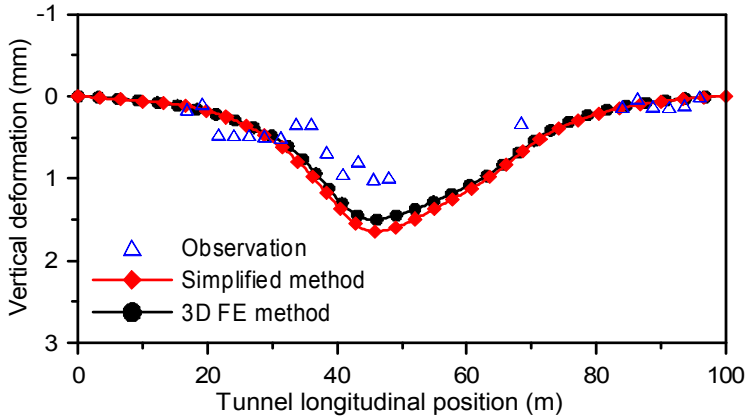

Fig. 14 Comparisons for tunnel vertical deformation after traversing completion for up- and down-line 11

solution are in good agreement with the numerical solution. In addition, the calculated sagging of the tunnel displacements is deeper than measured results and that the calculated maximum displacement is larger, which offers a conservative estimate of the tunnel deformation induced by overlapping tunneling. Generally speaking, the deformation curves calculated by the simplified theoretical method and the 3D FE numerical method are in general consistent with the in-situ monitoring date, which suggests that both the simplified theoretical method and the 3D FE numerical method can effectively analyze the deformation of existing tunnels induced by overlapping tunneling.

6. Deformation controlling technical measurements

6.1 Earth pressure for cutting open

In order to optimize the shield operation parameters to adapt the geology condition and to provide a reference for the overlapping crossing stage, the total distances of 30 rings from the 951th to the 980th ring of up- and down-line, respectively, are selected for shield propelling trial before crossing construction. Fig. 15 shows the soil settlements ahead by cutting open for up- and down-line propulsion trial stage. For the trial results of the up-line shield propulsion, when the soil lateral pressure coefficient is 0.85, the soil settlement value ahead by cutting open from 976th to 980th ring is within the range of -0.09 mm to -0.03 mm. It is clear that the soil disturbance is comparatively small with a small amount of soil upheaval. According to the crossing stage, the soil lateral pressure coefficient of the up-line shield is 0.85, and the initial soil pressure by cutting open is 0.37 MPa based on the trial stage data. Similarly, in regard to the trial results of the down-line shield propulsion, when the soil lateral pressure coefficient is 0.75, the soil settlement value ahead by cutting open from 976th to 980th ring is within the range of -0.07 mm to 0.04 mm. Therefore, the soil lateral pressure coefficient of the down-line shield is 0.75, and the initial soil pressure by cutting open is 0.13 MPa in the crossing stage.

According to the overlapping crossing construction stage, based on shield machine data acquisition system and in-site monitoring results, the soil pressure ahead by cutting open is dynamic slightly adjusted within 0.01 MPa each time, which ensures that soil body ahead by cutting open could have a small amount of upheaval and the soil pressure could have dynamic equilibrium during the process of shield propulsion.

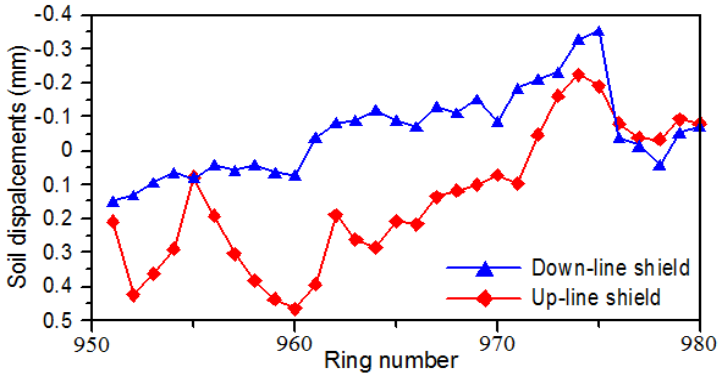

Fig. 15 Soil settlements ahead by cutting open for propulsion trial stage

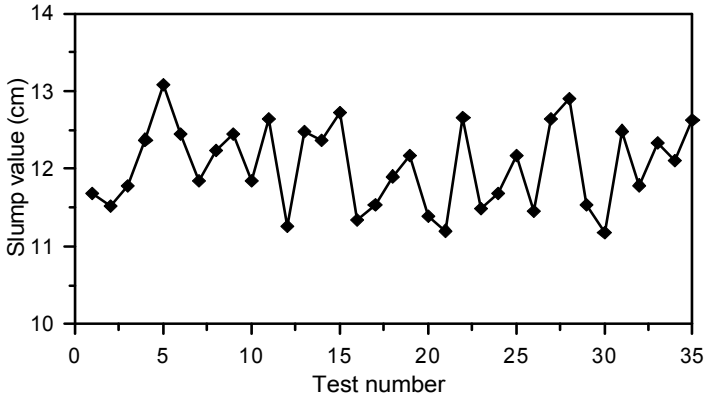

Fig. 16 Slump test results for slurry

6.2 Synchronized grouting

In order to enhance grouting capability of the shield machine, to reduce the ground loss caused by the physical gap between the outer diameter of shield machine and segment lining, and at the same time to reduce disturbance impacts on the nearby line 4, six grouting holes are drilled in both the shield waist and shield tail additionally, which are distributed evenly along the circumference and sealed with a high-quality ball valve. Meanwhile, in order to effectively control the synchronized grouting volume and to get uniform pressure injection, the multiple-points rotation grouting method is applied at overlapping crossing stage. Considering that the propulsion distance of each shield ring is 1200 mm, two grouting holes that are diagonal and nearby are set as a group, and one rotation is conducted every 300 mm.

In this project, the slurry in the synchronous grouting system has the obvious advantage of large density, low viscosity and little shrinkage. In order to improve the slurry quality, the slurry is unified mixed by the concrete batching station and the slurry sample is reserved at the construction site. The results of the slump tests in the overlapping crossing stage are shown in Fig. 16. It can be seen that the value for the slurry slump is within the range of 11 cm to 13.5 cm, which satisfies with the standards of the retarding mortar.

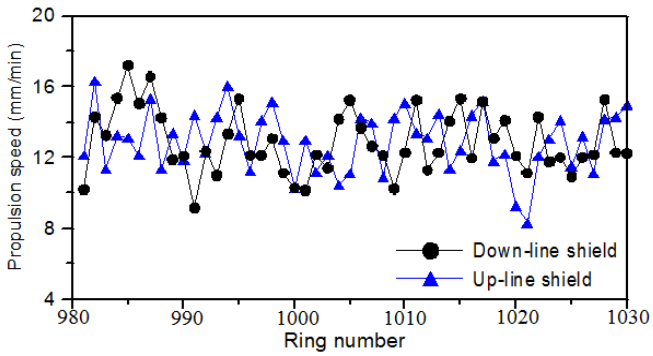

Fig. 17 Propulsion speed for shield crossing stage

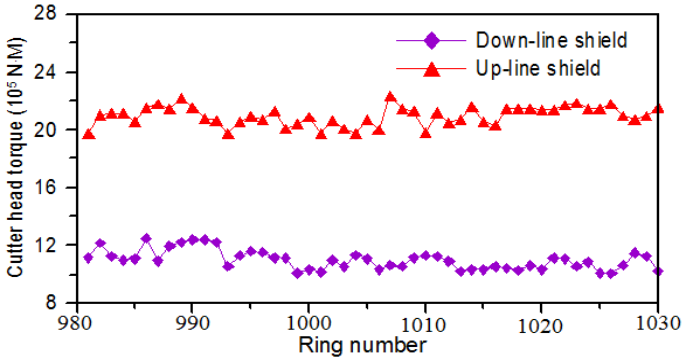

Fig. 18 Cutter head torque for shield crossing stage

6.3 Propulsion speed

Propulsion speed during tunneling construction should be reasonably set to keep the shield machine moving slowly forward at a uniform rate and to reduce the surrounding soils disturbance, so as to achieve reducing the deformation impacts on adjacent structures.

In this project, taking into account that the clear distance between the up-line shield and the line 4 is only 1.82 m and the clear distance between the down-line shield and the line 4 is only 1.69 m, the shield propulsion speed should be adjusted in plan based on monitoring data to reduce the ultra-close construction risk. For example, first propelled half ring distance (60 cm), paused 10 ~ 20 min, and then propelled the other half ring distance (60 cm) after the propulsion speed adjustment based on the deformation data of line 4 from. Fig. 17 shows the setting of propulsion speeds for up-line and down-line 11 during the crossing process. It can be seen from the figure, shield propulsion speeds are substantially controlled within a range of 10~15 mm/min to keep the speed stability and reduce the construction disturbance impacts on the nearby line 4.

6.4 Cutter head and screw machine torque

In the crossing region of this project, the up-line shield crossed below the line 4 is located in the ⑤$_1$ clay layer and ⑤$_3$ silty clay layer, while the down-line shield crossed above the line 4 is located in the ③ muddy silty clay layer and ④ muddy clay layer. Thus the soil strata of crossing region for the up-line and down-line shield are very complex. Therefore, it is necessary to pay attention to the setting parameters, such as, cutter head and screw machine torques, and to apply dynamic adjustments.

Based on the setting parameters of trial propulsion stage and taking into account the up-line shield is buried deeper, the cutter head torque is set between 2000~2300 KN·m; while since the down-line is buried shallower, the cutter head torque is set between 1000~1300 KN·m. The cutter head torque in the shield overlapping crossing stage is shown in Fig. 18. In actual operation process, when the cutter head torque or the oil pressure of screw machine is comparatively large, the bentonite slurry or water can be injected to the cutter head or screw machine by mud pump.

7. Conclusions

This paper presents the tunneling construction history of the second-stage north route of Shanghai railway transportation line 11. Considering the sheltering effects of existing tunnels of line 4 during crossing above and below process, the soil sheltering displacements and the deformation of existing tunnels caused by shield tunneling are presented by using the simplified theoretical method, the 3D FE numerical simulation method, and the in-situ monitoring method.

- The simplified theoretical analyses for the sheltering soil displacements are based on the modified stochastic medium method and the Powell's optimization procedure. The modified stochastic medium method can not only consider the ground surface settlements, but also consider the arbitrary subsoil movements.
- The simplified theoretical analyses for the deformation of existing tunnels are based on the Winkler foundation and Galerkin method.
- The 3D FE numerical simulation method can fully consider the shield propulsion, shield tail grouting, lining construction and slurry harden process. The good agreements are obtained between the results of simplified theoretical method and those of the 3D FE numerical method.
- The analyses results show that the stiffness of existing underground structures is one of the main factors affecting the degree of sheltering effects. The value of soil movements considering free displacement field is obviously different with the value considering the sheltering effects of existing structures. It is indicated that the sheltering effects of existing structures have a greater influence on the soil movements caused by the shield construction, which should be given to emphatic consideration in the theoretical analyses.

Acknowledgments

The research described in this paper was financially supported by the Natural Science Foundation of China (No. 51008188 and No. 41172238), and by the Shanghai Natural Science Foundation (No. 15ZR1429400), and by the Open Project Program of State Key Laboratory of Geohazard Prevention and Geoenvironment Protection (No. SKLGP2015K015), and by the Open Project Program of Key Laboratory of Geohazard Prevention of Hilly Mountains, Ministry of Land and Resources (No. 2015k005).

References

Addenbrooke, T.I. and Potts, D.M. (2001), "Twin tunnel interaction: surface and subsurface effects", *Int. J. Geomech.*, **1**(2), 249-271.

Bobet, A. (2001), "Analytical solutions for shallow tunnels in saturated ground", *J. Eng. Mech.*, **127**(12), 1258-1266.

Bobet, A. (2010), "Drained and undrained response of deep tunnels subjected to far-field shear loading", *Tunn. Undergr. Space Technol.*, **25**(1), 21-31.

Byun, G.W., Kim, D.G. and Lee, S.D. (2006), "Behavior of the ground in rectangularly crossed area due to tunnel excavation under the existing tunnel", *Tunn. Undergr. Space Technol.*, **21**(3-4), 361-367.

Chehade, F.H. and Shahrour, I. (2008), "Numerical analysis of the interaction between twin-tunnels: influence of the relative position and construction procedure", *Tunn. Undergr. Space Technol.*, **23**(2), 210-214.

Chou, W.I. and Bobet, A. (2002), "Prediction of ground deformations in shallow tunnels in clay", *Tunn. Undergr. Space Technol.*, **17**(l), 3-19.
Dang, H.K. and Meguid, M.A. (2008), "Application of a multilaminate model to simulate the undrained response of structured clay to shield tunneling", *Can. Geotech. J.*, **45**(1), 14-28.
Do, N., Dias, D., Oreste, P. and Djeran-Maigre, I. (2014), "Three-dimensional numerical simulation for mechanized tunnelling in soft ground: the influence of the joint pattern", *Acta Geotech.*, **9**(4), 673-694.
Gui, M.W. and Chen, S.L. (2013), "Estimation of transverse ground surface settlement induced by DOT shield tunneling", *Tunn. Undergr. Space Technol.*, **33**(1), 119-130.
Kim, S.H., Burd, H.J. and Milligan, G.W.E. (1998), "Model testing of closely spaced tunnels in clay", *Geotechnique*, **48**(3), 375-388.
Klar, A., Vorster, T.E.B., Soga, K. and Mair, R.J. (2005), "Soil-pipe interaction due to tunnelling: comparison between Winkler and elastic continuum solutions", *Geotechnique*, **55**(6), 461-466.
Klar, A., Vorster, T.E.B., Soga, K. and Mair, R.J. (2007), "Elastoplastic solution for soil-pipe-tunnel interaction", *J. Geotech. Geoenviron. Eng.*, **133**(7), 782-792.
Klar, A., Marshall, A.M., Soga, K. and Mair, R.J. (2008), "Tunneling effects on jointed pipelines", *Can. Geotech. J.*, **45**(1), 131-139.
Lee, K.M., Rowe, R.K. and Lo, K.Y. (1992), "Subsidence owing to tunneling I: Estimating the gap parameter", *Can. Geotech. J.*, **29**(6), 929-940.
Lee, C.J., Wu, B.R., Chen, H.T. and Chiang, K.K. (2006), "Tunnel stability and arching effects during tunneling in soft clayey soil", *Tunn. Undergr. Space Technol.*, **21**(2), 119-132.
Li, P., Du, S.J., Ma, X.F., Yin, Z.Y. and Shen, S.L. (2014), "Centrifuge investigation into the effect of new shield tunnelling on an existing underlying large-diameter tunnel", *Tunn. Undergr. Space Technol.*, **42**(5), 59-66.
Liu, B.C. (1993), *Ground Surface Movements Due to Underground Excavation in the PR China*, Pergamon Press, Oxford, UK.
Liu, H.Y., Small, J.C., Carter, J.P. and Williams, D.J. (2009), "Effects of tunnelling on existing support systems of perpendicularly crossing tunnels", *Comput. Geotech.*, **36**(5), 880-894.
Loganathan, N. and Poulos, H.G. (1998), "Analytical prediction for tunneling-induced ground movements in clays", *J. Geotech. Geoenviron. Eng.*, **124**(9), 846-856.
Marshall, A.M., Klar, A. and Mair, R.J. (2010), "Tunneling beneath buried pipes: view of soil strain and its effect on pipeline behavior", *J. Geotech. Geoenviron. Eng.*, **136**(12), 1664-1672.
Mašín, D. (2009), "3D modeling of an NATM tunnel in high K_0 clay using two different constitutive models", *J. Geotech. Geoenviron. Eng.*, **135**(9), 1326-1335.
Ng, C.W.W., Lee, K.M. and Tang, D.K.W. (2004), "Three-dimensional numerical investigations of new Austrian tunnelling method (NATM) twin tunnel interactions", *Can. Geotech. J.*, **41**(3), 523-539.
Ng, C.W.W., Boonyarak, T. and Mašín, D. (2013), "Three-dimensional centrifuge and numerical modeling of the interaction between perpendicularly crossing tunnels", *Can. Geotech. J.*, **50**(9), 935-946.
Park, K.H. (2004), "Elastic solution for tunneling-induced ground movements in clays", *Int. J. Geomech.*, **4**(4), 310-318.
Park, K.H. (2005), "Analytical solution for tunneling-induced ground movement in clays", *Tunn. Undergr. Space Technol.*, **20**(3), 249-261.
Peck, R.B. (1969), "Deep excavation and tunneling in soft ground", *Proceedings of 7th International Symposium on Soil Mechanics Foundation Engineering*, Mexico City, Mexico, June.
Thomas, K. and Gunther, M. (2006), "A numerical study of the effect of soil and grout material properties and cover depth in shield tunneling", *Comput. Geotech.*, **33**(4-5), 234-247.
Verruijt, A. and Booker, J.R. (1996), "Surface settlements due to deformation of a tunnel in an elastic half plane", *Geotechnique*, **46**(4), 753-756.
Vesic, A.B. (1961), "Bending of beams resting on isotropic elastic solids", *J. Eng. Mech.*, **87**(2), 35-53.
Vorster, T.E.B., Mair, R.J., Soga, K. and Klar, A. (2005a), "Centrifuge modelling of the effects of tunnelling on buried pipelines: mechanisms observed", *Proceedings of the 5th International Symposium on Geotechnical Aspects of Underground Construction in Soft Ground*, Amsterdam, The Netherlands, June.

Vorster, T.E.B., Klar, A., Soga, K. and Mair, R.J. (2005b), "Estimating the effects of tunneling on existing pipelines", *J. Geotech. Geoenviron. Eng.*, **131**(11), 1399-1410.
Wang, Y., Shi, J.W. and Ng, C.W.W. (2011), "Numerical modeling of tunneling effect on buried pipelines", *Can. Geotech. J.*, **48**(7), 1125-1137.
Yang, X.L. and Wang, J.M. (2011), "Ground movement prediction for tunnels using simplified procedure", *Tunn. Undergr. Space Technol.*, **26**(3), 462-471.
Yang, J.S., Liu, B.C. and Wang, M.C. (2004), "Modeling of tunneling-induced ground surface movements using stochastic medium theory", *Tunn. Undergr. Space Technol.*, **19**(2), 113-123.
Zhang, Z.G., Huang, M.S. and Zhang, M.X. (2011), "Theoretical prediction of ground movements induced by tunnelling in multi-layered soils", *Tunn. Undergr. Space Technol.*, **26**(2), 345-355.
Zhang, Z.G., Zhang, M.X., Wang, W.D. and Xi, X.G. (2014), "Tunneling-induced ground movements in clays considering oval-shaped convergence deformation pattern", *Proceedings of Geo-Shanghai 2014-Tunneling and Underground Construction*, Shanghai, China, May.

JS